

# Determination of the resistivity anisotropy of SrRuO<sub>3</sub> by measuring the planar Hall effect

Isaschar Genish and Lior Klein

*Department of Physics, Bar-Ilan University, Ramat-Gan 52900, Israel*

James W. Reiner\* and M. R. Beasley

*T. H. Geballe Laboratory for Advanced Materials, Stanford University, Stanford, California 94305, USA*

(Received 7 September 2006; revised manuscript received 7 December 2006; published 13 March 2007)

We have measured the planar Hall effect in epitaxial thin films of the itinerant ferromagnet SrRuO<sub>3</sub> patterned with their current paths at different angles relative to the crystallographic axes. Based on the results, we have determined that SrRuO<sub>3</sub> exhibits small resistivity anisotropy in the entire temperature range of our measurements (between 2 and 300 K); namely, both above and below its Curie temperature (150 K). Our results indicate that in addition to anisotropy related to the spontaneous magnetization, the resistivity anisotropy of SrRuO<sub>3</sub> has an intrinsic, nonmagnetic source. We have found that the two sources of anisotropy have competing effects.

DOI: [10.1103/PhysRevB.75.125108](https://doi.org/10.1103/PhysRevB.75.125108)

PACS number(s): 73.50.Jt, 75.30.Gw

## I. INTRODUCTION

The itinerant ferromagnet SrRuO<sub>3</sub> has attracted considerable experimental and theoretical effort for its intriguing properties, including “bad metal” behavior,<sup>1,2</sup> deviation from normal metal optical conductivity,<sup>3</sup> high sensitivity to disorder,<sup>4</sup> and negative deviation from Matthiessen’s rule.<sup>5</sup> Consequently, there is growing interest in obtaining comprehensive characterization of its properties and, in particular, its transport behavior. Here, we address a basic transport feature of SrRuO<sub>3</sub> as we use planar-Hall-effect measurements to determine quantitatively the existence of spontaneous resistivity anisotropy.

Being almost cubic, the few indications for spontaneous resistivity anisotropy in SrRuO<sub>3</sub> have been subtle and qualitative; for example, resistivities measured along [001] and [1 $\bar{1}$ 0] exhibit different critical behavior and they also seem to have slightly different values in the paramagnetic state.<sup>1</sup> These small differences imply that even if the anisotropy is real (and not due to spurious effects), it does not exceed a few percent; hence, its quantitative determination is challenging.

In principle, obtaining quantitative characterization of spontaneous resistivity in a conductor can be achieved by direct measurements of the resistivity for different current directions. This method, however, is not very useful when the anisotropy is on the order of a few percent, since it is affected by other sources (e.g., variations in geometrical factors and in the number and type of defects), whose contribution could be on the order of that of the intrinsic anisotropy. To overcome this difficulty, we deduce the intrinsic spontaneous resistivity anisotropy in SrRuO<sub>3</sub> by measuring the planar Hall effect (PHE) of this compound.

The PHE (Refs. 6–8) is the appearance of transverse resistivity  $\rho_{xy}$  observed in conductors with resistivity anisotropy. In magnetic compounds, it is usually related to the anisotropic magnetoresistance<sup>8</sup> which is the dependence of the longitudinal resistivity  $\rho_{xx}$  on the angle  $\theta$  between the current and the internal magnetization. For many compounds, it is found that

$$\rho_{xx} = \rho_{\perp} + (\rho_{\parallel} - \rho_{\perp})\cos^2 \theta$$

and

$$\rho_{xy} = (\rho_{\parallel} - \rho_{\perp})\cos \theta \sin \theta,$$

where  $\rho_{\parallel}$  and  $\rho_{\perp}$  are the resistivities with the magnetization parallel and perpendicular to the current, respectively. However, simply measuring the transverse resistivity is also not sufficient since misalignment of contact leads would introduce a regular longitudinal contribution that is hard to distinguish from the transverse signal, since contrary to ordinary and extraordinary Hall effects, the planar Hall effect is symmetric under magnetization reversal, as is the longitudinal resistivity. Therefore, for reliable determination of the PHE, one needs to demonstrate the expected dependence of the PHE on the angle between the current path and the principal axes of the resistivity tensor.

Despite being commonly associated with magnetism, PHE is a phenomenon which arises whenever there is resistivity anisotropy and the current is not along one of the principal axes of the resistivity tensor; hence, it can be used to directly determine the intrinsic anisotropy of a conductor irrespective of the source of the anisotropy, including a nonmagnetic source. However, if a nonmagnetic source of the anisotropy exists, one cannot rotate the direction of the principal axes of the resistivity tensor by changing the direction of an applied magnetic field. Therefore, we “rotate” the current path relative to the crystallographic axes by patterning current paths in different directions. Using this method, we have quantitatively determined the resistivity anisotropy of SrRuO<sub>3</sub> both above and below the Curie temperature and we have found that the anisotropy has both magnetic and nonmagnetic sources with competing effects. The success of this method indicates that it could be a useful method for determining subtle anisotropy of other conductors as well.

## II. MEASUREMENTS AND DISCUSSION

Our samples are epitaxial films of SrRuO<sub>3</sub> grown on slightly miscut (2°) SrTiO<sub>3</sub>. The films are orthorhombic (*a*

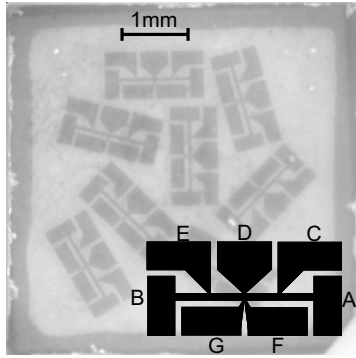


FIG. 1. Photo of the measured sample which consists of eight patterns at different orientations. Inset: a scheme of an individual pattern.

$a=5.53 \text{ \AA}$ ,  $b=5.57 \text{ \AA}$ , and  $c=7.85 \text{ \AA}$ ) (Ref. 9) and their Curie temperature is  $\sim 150 \text{ K}$ . The films grow with the in-plane  $c$  axis perpendicular to the miscut, and  $a$  and  $b$  axes at  $45^\circ$  relative to the film plane. The films exhibit uniaxial magnetocrystalline anisotropy with the easy axis close to the  $b$  axis.<sup>9</sup> These are twin-free films whose high quality has been previously manifested, including in exhibiting low-temperature magnetoresistance quantum oscillations.<sup>10</sup>

The data presented here are from a 27-nm-thick film with a resistivity ratio of  $\sim 12$  on which there are eight identical patterns, each along a different crystallographic direction in the (110) plane. The angles of the patterns relative to the  $[1\bar{1}0]$  axis (in the film plane) are  $-45^\circ$ ,  $0^\circ$ ,  $15^\circ$ ,  $30^\circ$ ,  $45^\circ$ ,  $60^\circ$ ,  $75^\circ$ , and  $90^\circ$ . Each pattern allows longitudinal and transverse resistivity measurements (see Fig. 1).

The resistance measured between the pads marked F and D  $R_{FD}$  has several contributions: (a) longitudinal resistance due to longitudinal shift between the two leads, (b) ordinary Hall effect (OHE) and extraordinary Hall effect<sup>11</sup> (EHE) due to magnetic field and magnetization, and (c) PHE. According to the pattern design, the longitudinal resistance should be half the resistance between F and G  $R_{FG}$ ; therefore, it can be subtracted. The OHE and EHE are antisymmetric signals, and they are determined by interchanging current and voltage leads.<sup>12</sup> Figure 2(a) shows  $R_{FD}$  as a function of temperature for all the patterns. The measurements are at zero applied field after field cooling to avoid contribution of magnetic domain walls to resistivity.<sup>13</sup> The antisymmetric contribution to  $R_{FD}$  (obtained by current and voltage interchange) for all the patterns is shown in Fig. 2(b). Since the applied field is zero, the obtained signal is the EHE. We see that this contribution is almost identical for all patterns (and consistent with previous reports<sup>14</sup>) indicating that, as expected, only the perpendicular component of the magnetization, which is identical for all patterns, is relevant. In Fig. 2(c), we show the PHE for all the patterns after subtracting the antisymmetric part and the expected contribution due to longitudinal resistance.

We note that the PHE curves exhibit similar qualitative temperature dependence. The largest PHE is obtained for  $\theta = \pm 45^\circ$ , while the smallest is obtained for  $\theta = 0^\circ$  and  $90^\circ$ . This indicates that the resistivities in the  $0^\circ$  and  $90^\circ$  directions,  $\rho_0$  and  $\rho_{90}$ , are the principal axes of resistivity, and we

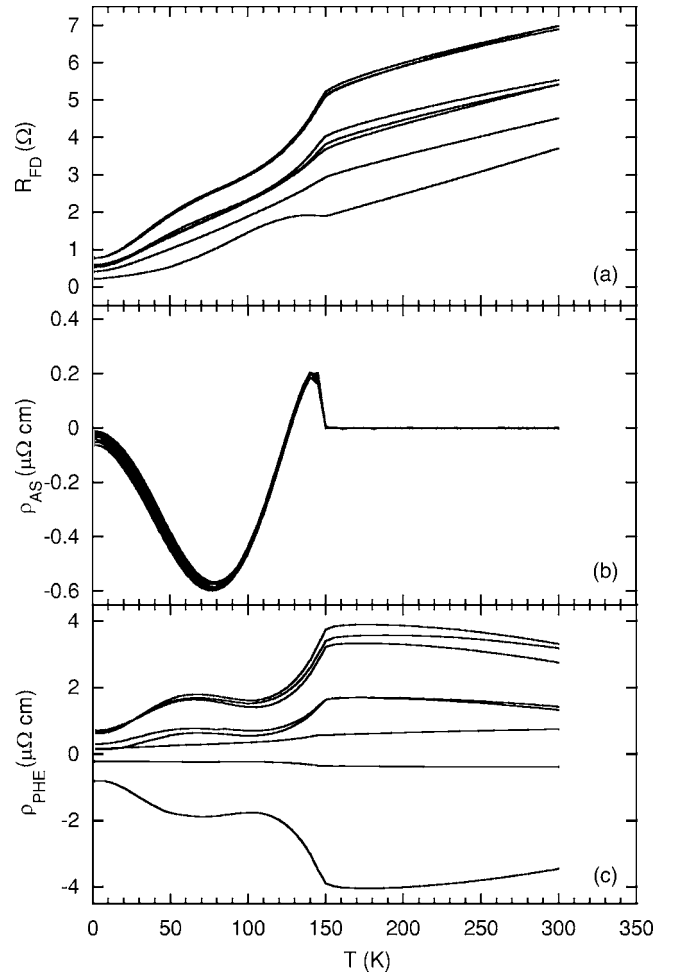


FIG. 2. (a)  $R_{FD}$  as a function of temperature for the eight patterns. In decreasing order of  $R_{FD}$  value at 300 K, the curves correspond to patterns at angles of  $45^\circ$ ,  $30^\circ$ ,  $15^\circ$ ,  $0^\circ$ ,  $75^\circ$ ,  $90^\circ$ , and  $-45^\circ$ . (b) The antisymmetric contribution to  $R_{FD}$ . (c) PHE contribution to  $R_{FD}$ . In decreasing order of their value at 300 K, the curves correspond to patterns at angles of  $45^\circ$ ,  $60^\circ$ ,  $30^\circ$ ,  $15^\circ$ ,  $75^\circ$ ,  $0^\circ$ ,  $90^\circ$ , and  $-45^\circ$ .

expect that at each temperature the PHE for current in the  $\theta$  direction will obey  $\rho_{xy} = (\rho_0 - \rho_{90}) \sin \theta \cos \theta$ . It also means that between any two PHE curves obtained for patterns at angles  $\theta_1$  and  $\theta_2$ , there will be temperature-independent proportionality given by  $\cos \theta_1 \sin \theta_1 / \cos \theta_2 \sin \theta_2$ .

As noted above, the longitudinal resistance contribution to  $R_{FD}$  should be  $a \times R_{FG}$  with  $a=0.5$ . However, minute lithography variations may slightly change this factor. If the correct longitudinal contribution is precisely determined for all angles, we expect that all the PHE curves will be proportional to each other. Therefore, we use MATLAB for refining  $a$  within a few percent in order to obtain the simultaneously best proportionality between the data sets of PHE obtained for the different angles. The process does not impose the magnitude of the proportionality factor. Figure 3(a) shows the PHE for all the angles after the refinement. To show the proportionality, we present in Fig. 3(b) the PHE at various angles as a function of the PHE obtained for  $\theta=45^\circ$ . The inset of Fig. 3(b) shows the proportionality factor as a func-

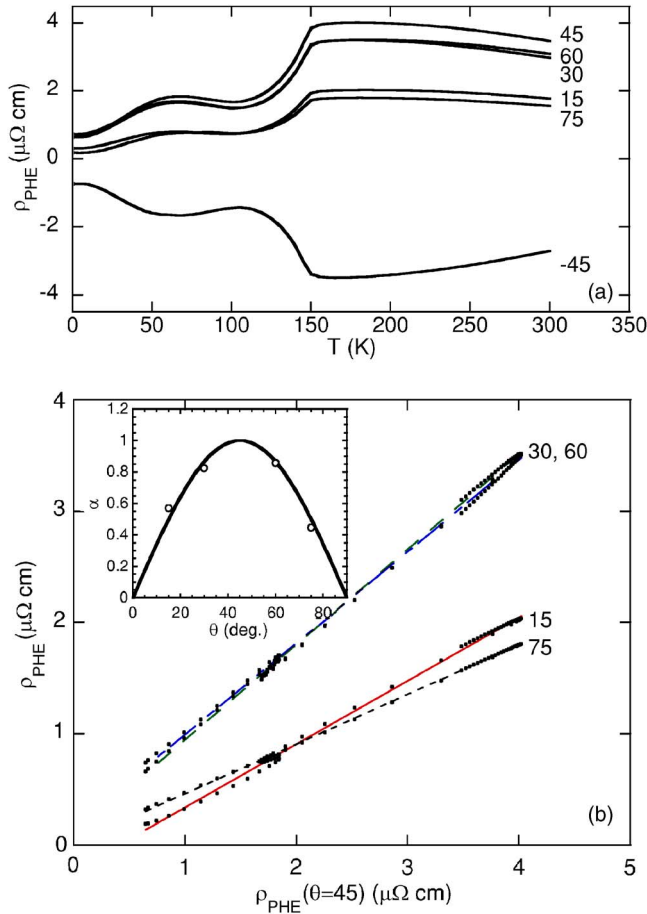


FIG. 3. (Color online) (a) Refined PHE (see text) vs temperature. The number near the curve indicates the pattern orientation. (b) The PHE in patterns oriented at various angles vs the PHE in the pattern oriented at 45°. The lines are linear fits. Inset: the slope of the linear fits  $\alpha$  as a function of  $\theta$ . The line is the expected  $\sin \theta \cos \theta$  dependence.

tion of the pattern angle where the solid line is  $\sin \theta \cos \theta$  (with no adjustable parameters). This remarkable consistency obtained between all PHE curves strongly supports the reliability of the obtained PHE curve.

Figure 4 presents the resistivity anisotropy as obtained from the PHE. The results show that in the entire temperature range of our measurements (2–300 K),  $\rho_0$  (along  $[110]$ ) is larger than  $\rho_{90}$  (along  $[001]$ ). As a consistency check, we show that if we allow for small adjustments of a few percent, we can correlate the PHE with the difference between  $\rho_{xx}$  measured at different angles. The agreement is very satisfactory in view of the effect of other sources on the variations between different patterns, such as different defect concentration. It should be noted that only the fact that we have determined the anisotropy by PHE measurements allowed us to make the small adjustments in the longitudinal resistivities.

What are the sources of the resistivity anisotropy that we have determined? Clearly, a significant source is related to the magnetization which breaks the symmetry of the transport properties regarding magnetic-related scattering. However, since  $\text{SrRuO}_3$  is an orthorhombic perovskite, the band

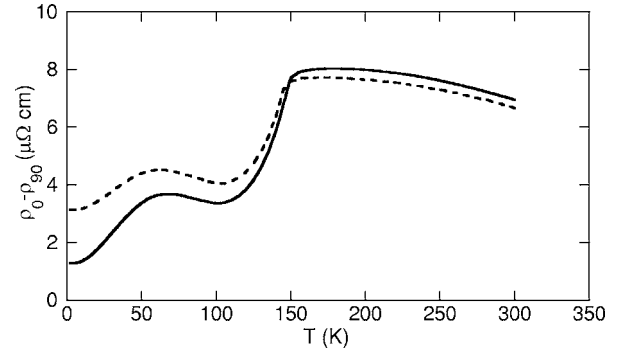


FIG. 4. The anisotropy  $\rho_0 - \rho_{90}$  as determined by PHE measurements (continues) and from subtraction of longitudinal resistivities (dashed).

structure itself is anisotropic with different Fermi velocities along the principle crystal axes; hence, even without considering the effect of magnetic-related scattering, anisotropic resistivity is expected.

To identify the effect of the different sources of the anisotropy, we examine the anisotropy in the paramagnetic state. Despite the lack of spontaneous magnetization, we cannot exclude *a priori* the possibility that anisotropic spin fluctuations are responsible for the observed anisotropy, particularly in view of the observed anisotropic paramagnetic susceptibility that we have reported before.<sup>15</sup> Therefore, the first question we ask is whether this anisotropy can be attributed to magnetic scattering.

In Fig. 5, we show the change in PHE (namely, the anisotropy) few degrees above the Curie temperature when a field of 8 T is rotated in the film plane of a pattern oriented at 45°. The horizontal line indicates the PHE value when no field is applied. We first notice that when the field is at angles exactly in between the two principle axes of the resistivity ( $\pm 45^\circ$ ), there is no observable change in the anisotropy, despite significant suppression of spin fluctuations. This indicates that anisotropic spin fluctuations cannot account for the resistivity anisotropy. In addition, we see that when the field is rotated in the film plane there are symmetric variation

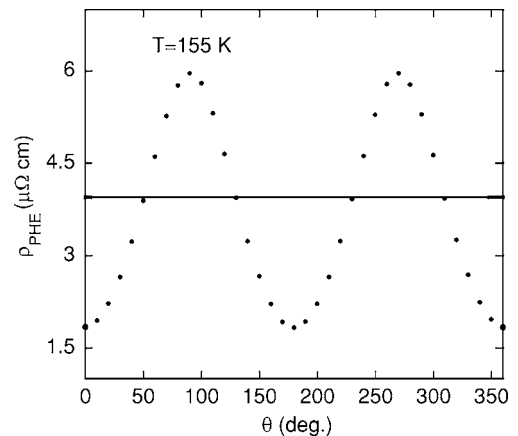


FIG. 5. The PHE for the pattern oriented at 45° at 155 K as a function of  $\theta$ , the angle between an in-plane 8 T field and  $[1\bar{1}0]$ . The dashed line is the zero field value of the PHE.

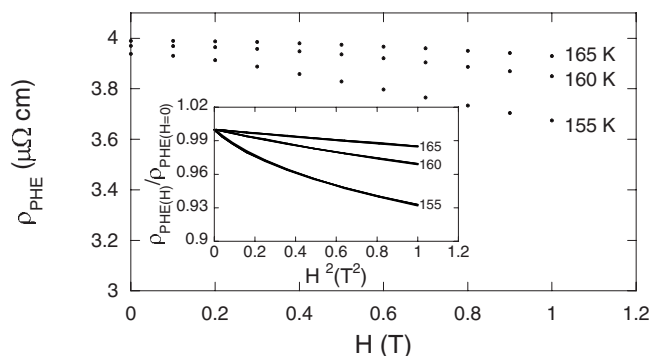


FIG. 6. The PHE for the  $45^\circ$  oriented pattern vs  $H$  applied along the  $b$  axis at 155, 160, and 165 K. Inset: PHE normalized by its zero-field value as a function of  $H^2$  at 155, 160, and 165 K. At each temperature, the data for all the patterns are presented; however, due to scaling, the data points are undistinguishable.

above and below the zero-field line. This indicates that the dominant source of anisotropy in the paramagnetic state is not related to magnetic scattering. This observation is qualitatively consistent with band calculations of  $\text{SrRuO}_3$  which find anisotropic Fermi velocities in the paramagnetic state.<sup>16</sup>

Figure 6 shows the effect of applying a magnetic field in the paramagnetic state along the  $b$  axis which is the easy axis of magnetization. We see that the PHE decreases as the induced magnetization increases. The inset shows the relative change in the PHE for all patterns as a function of  $H^2$ . We note that all patterns show the same field dependence, as expected from the fact that all PHE values are related by temperature-independent and field-independent constants. At higher temperatures, we see also that the magnetically re-

lated anisotropy is proportional to  $H^2$ , namely, to  $M^2$ . The fact that the induced magnetization decreases the PHE indicates that it has an opposite effect to that of the nonmagnetic source. In view of this observation, the sharp decrease in the zero-field PHE when temperature decreases below  $T_C$  is understood as a result of the onset of spontaneous magnetization.

In the paramagnetic state, we see a gradual decrease of the PHE with increasing temperature. As discussed above, this anisotropy is probably related to the deviation from cubic structure. Studies have shown that  $\text{SrRuO}_3$  films grown on  $\text{SrTiO}_3$  undergo two structural phase transitions, orthorhombic to tetragonal at  $\sim 350^\circ\text{C}$  and tetragonal to cubic at  $\sim 600^\circ\text{C}$ .<sup>17</sup> Therefore, we expect  $600^\circ\text{C}$  to be the upper limit for the observed anisotropy.

### III. CONCLUSIONS

By measuring the planar Hall effect on patterns with current paths oriented at different crystallographic directions, we were able to determine both magnetic and nonmagnetic sources of anisotropy present in epitaxial films of  $\text{SrRuO}_3$ . We find that the in-plane principal axes are  $[1\bar{1}0]$  and  $[001]$  and that nonmagnetic anisotropy makes the resistivity along  $[1\bar{1}0]$  larger, while spontaneous magnetization (along  $[010]$ ) decreases this anisotropy.

### ACKNOWLEDGMENT

This research was supported by The Israel Science Foundation founded by the Israel Academy of Sciences and Humanities.

\*Present address: Department of Applied Physics, Yale University, New Haven, Connecticut 06520-8284.

<sup>1</sup>L. Klein, J. S. Dodge, C. H. Ahn, G. J. Snyder, T. H. Geballe, M. R. Beasley, and A. Kapitulnik, *Phys. Rev. Lett.* **77**, 2774 (1996).

<sup>2</sup>M. S. Laad and E. Müller-Hartmann, *Phys. Rev. Lett.* **87**, 246402 (2001); Carsten Timm, M. E. Raikh, and Felix von Oppen, *ibid.* **94**, 036602 (2005).

<sup>3</sup>P. Kostic, Y. Okada, N. C. Collins, Z. Schlesinger, J. W. Reiner, L. Klein, A. Kapitulnik, T. H. Geballe, and M. R. Beasley, *Phys. Rev. Lett.* **81**, 2498 (1998); J. S. Dodge, C. P. Weber, J. Corson, J. Orenstein, Z. Schlesinger, J. W. Reiner, and M. R. Beasley, *ibid.* **85**, 4932 (2000).

<sup>4</sup>L. Capogna, A. P. Mackenzie, R. S. Perry, S. A. Grigera, L. M. Galvin, P. Raychaudhuri, and A. J. Schofield, C. S. Alexander, G. Cao, S. R. Julian, and Y. Maeno, *Phys. Rev. Lett.* **88**, 076602 (2002).

<sup>5</sup>L. Klein, Y. Kats, N. Wisser, M. Konczykowski, J. W. Reiner, T. H. Geballe, M. R. Beasley, and A. Kapitulnik, *Europhys. Lett.* **55**, 532 (2001).

<sup>6</sup>C. Goldberg and R. E. Davis, *Phys. Rev.* **94**, 1121 (1954); F. G. West, *J. Appl. Phys.* **34**, 1171 (1963).

<sup>7</sup>W. M. Bullis, *Phys. Rev.* **109**, 292 (1958).

<sup>8</sup>I. A. Campbell, *Phys. Rev. Lett.* **24**, 269 (1970); I. A. Campbell,

A. Fert, and O. Jaoul, *J. Phys. C* **3**, S95 (1970); T. R. McGuire and R. I. Potter, *IEEE Trans. Magn.* **11**, 1018 (1975).

<sup>9</sup>A. F. Marshall, L. Klein, J. S. Dodge, C. H. Ahn, J. W. Reiner, L. Mieville, L. Antognazza, A. Kapitulnik, T. H. Geballe, and M. R. Beasley, *J. Appl. Phys.* **85**, 4131 (1999).

<sup>10</sup>A. P. Mackenzie, J. W. Reiner, A. W. Tyler, L. M. Galvin, S. R. Julian, M. R. Beasley, T. H. Geballe, and A. Kapitulnik, *Phys. Rev. B* **58**, R13318 (1998).

<sup>11</sup>J. Smit, *Physica (Amsterdam)* **21**, 877 (1955); J. M. Luttinger, *Phys. Rev.* **112**, 739 (1958); J. Smit, *Physica (Amsterdam)* **24**, 39 (1958); L. Berger, *Phys. Rev. B* **2**, 4559 (1970).

<sup>12</sup>M. Büttiker, *Phys. Rev. Lett.* **57**, 1761 (1986).

<sup>13</sup>L. Klein, Y. Kats, A. F. Marshall, J. W. Reiner, T. H. Geballe, M. R. Beasley, and A. Kapitulnik, *Phys. Rev. Lett.* **84**, 6090 (2000); M. Feigenson, L. Klein, J. W. Reiner, and M. R. Beasley, *Phys. Rev. B* **67**, 134436 (2003).

<sup>14</sup>M. Izumi, K. Nakazawa, Y. Bando, Y. Yoneda, and H. Terauchi, *J. Phys. Soc. Jpn.* **66**, 3893 (1997); L. Klein, J. W. Reiner, T. H. Geballe, M. R. Beasley, and A. Kapitulnik, *Phys. Rev. B* **61**, R7842 (2000); Z. Fang, N. Nagaosa, K. S. Takahashi, A. Asamitsu, R. Mathieu, T. Ogasawara, H. Yamada, M. Kawasaki, Y. Tokura, and K. Terakura, *Science* **302**, 92 (2003);

- R. Mathieu, C. U. Jung, H. Yamada, A. Asamitsu, M. Kawasaki, and Y. Tokura, *Phys. Rev. B* **72**, 064436 (2006).
- <sup>15</sup>Y. Kats, I. Genish, L. Klein, J. W. Reiner, and M. R. Beasley, *Phys. Rev. B* **71**, 100403(R) (2005).
- <sup>16</sup>P. B. Allen, H. Berger, O. Chauvet, L. Forro, T. Jarlborg, A. Junod, B. Revaz, and G. Santi, *Phys. Rev. B* **53**, 4393 (1996); D. J. Singh, *J. Appl. Phys.* **79**, 4818 (1996); G. Santi and T. Jarlborg, *J. Phys.: Condens. Matter* **9**, 9563 (1997).
- <sup>17</sup>J. P. Maria, H. L. McKinstry, and S. Trolrier-McKinstry, *Appl. Phys. Lett.* **76**, 3382 (2000).